Korean J. Chem. Eng., 33(11), 3273-3280 (2016)
DOI: 10.1007/s11814-016-0199-y

pISSN: 0256-1115
eISSN: 1975-7220

A new polymeric additive as asphaltene deposition inhibitor in CO_2 core flooding

Sepideh Kashefi*, Abbas Shahrabadi, Mohammad Nader Lotfollahi*,†, and Akbar Varamesh*****

*Faculty of Chemical, Petroleum and Gas Engineering, Semnan University, Semnan 35131-19111, Iran
**Exploration and Production Division, Research Institute of Petroleum Industry (RIPI), Tehran 14665137, Iran
***Polymer Science and Technology Division, Research Institute of Petroleum Industry (RIPI), Tehran, Iran
(*Received 16 December 2015 • accepted 5 July 2016*)

Abstract−A new synthesized polymeric inhibitor (SPI) based on the poly-alkyl phenol formaldehyde and polyamine was introduced as asphaltene deposition inhibitor. A Turbiscan apparatus was used to investigate the stability of precipitated asphaltene in crude oil solutions by adding different concentrations of the SPI. The results of turbidity showed that the SPI could delay the asphaltene deposition and provide high stability of precipitated asphaltene in oil solutions. Then two dynamic experiments, including co-injection of crude oil and CO_2 into a sandstone core, were conducted with and without the use of 500 mg/L SPI at 173 bar and 50 °C. The permeability ratio and asphaltene content remained relatively unchanged throughout the core flooding with the use of SPI, which indicated increase of the asphaltene stability in the core sample. However, the permeability ratio and outlet asphaltene content in dynamic experiment without the use of SPI decreased by about 70% and 51%, respectively.

Keywords: Polymeric Inhibitor, Asphaltene Deposition, Crude Ool, CO_2 Injection, Core Flooding

INTRODUCTION

Enhanced oil recovery (EOR) is the process of increasing the amount of produced crude oil from a particular reservoir after the primary production. The EOR can be achieved by several techniques of thermal recovery [1], gas flooding [2] and chemical injection, which can involve the use of polymer [3], ionic liquid [4] and nanoparticle [5] to increase the efficiency of conventional water flooding.

CO_2 gas flooding has been an environmentally friendly method for enhancing oil recovery in oil fields and laboratory studies. This process can increase the efficiency of oil recovery by decreasing the oil viscosity and interfacial tension of oil [6,7]. Changes in the equilibrium conditions during CO_2 injection lead to the precipitation of organic solids such as asphaltenes in oil reservoirs. Asphaltenes are the heaviest fractions of crude oil with aliphatic and aromatic structures, which tend to have self-association and precipitation in solutions. Asphaltene precipitation and deposition can cause several problems during oil production, such as pore plugging, permeability reduction, wettability alteration, and consequently formation damage [8,9]. One effective method for decreasing the asphaltene precipitation and deposition is to use chemical additives. Several researchers have investigated the inhibition effects of various chemical additives such as amphiphiles [10-14], ionic liquids [15], vegetable oils [13], organic acids [12,13], and polymeric compounds [16-19] on asphaltene precipitation in ambient conditions. They have demonstrated that these additives interact with asphaltene particles [10-15] or are adsorbed on asphaltene surfaces [16-19] to prevent them from aggregation. Some investigators have studied the effects of asphaltene inhibitors at high pressure and high temperature during CO_2 injection in non-porous media. They have concluded that amphiphiles form a stable layer around the asphaltenes, depending on their head group's polarity and alkyl tail's length [20-22]. On the other hand, ionic liquids stop asphaltene associations due to their charge densities of the cation and anion in their structures [20]. Recently, the application of asphaltene inhibitors in porous media has been reported in few works. Alcázar-Vara et al. used a new class of zwitterionic liquids with co-acidic and basic properties as the asphaltene inhibitor under core flooding. They concluded that the use of this inhibitor could modify wettability and improve oil recovery [23]. Ghazvini et al. investigated the effects of different polar polyacrylamides on asphaltene deposition during dead oil flooding in porous media. They observed that the use of cationic and anionic polyacrylamide increased asphaltene deposition in porous media, but nonionic polyacrylamide inhibited the asphaltene precipitation [24]. Hashemi et al. used NiO nanoparticles as the asphaltene inhibitor during CO_2 injection into a core sample and found significant improvement in permeability reduction and asphaltene accumulation [25]. To our best knowledge, thus far, no research has been conducted on using polymeric asphaltene inhibitor during oil and CO_2 injection in porous media.

We synthesized a new polymeric asphaltene inhibitor based on the poly alkyl phenol formaldehyde and modified its structure by adding polyamine. The performance of the synthesized polymeric inhibitor (SPI) on stability of precipitated asphaltene in crude oil solution was studied by light turbidity method. Then, two dynamic experiments, including co-injection of oil and CO_2 into a sandstone core, were conducted in the absence and presence of the SPI at high pressure and high temperature. The effects of the SPI on asphaltene deposition, permeability, and porosity reduction in the porous media were also investigated.

†To whom correspondence should be addressed.
E-mail: mnlotfollahi@semnan.ac.ir, mnlotfollahi@yahoo.com

Table 1. Specifications of the dead oil sample[a]

Composition	%mol	Composition	%mol
C_1	0.00	C_6	13.81
C_2	0.07	C_7	10.50
C_3	0.45	C_8	8.06
i-C_4	0.95	C_9	11.76
n-C_4	4.63	C_{10}	7.81
i-C_5	2.89	C_{11}	7.86
n-C_5	3.39	C_{12+}[b]	27.82

[a]API=33.74, $\rho_{dead\ oil}$=0.8519 g/cm^3, $MW_{dead\ oil}$=216
[b]SG_{C12+}=0.8958, MW_{C12+}=508

Table 2. Petro-physical properties of the core sample

Test properties	E1	E2
Core type	Sandstone	Sandstone
Length (cm)	8.445	8.445
Diameter (cm)	3.73	3.73
Initial porosity (%)	10	10
Absolute permeability (md)	3.18	3.10
Initial oil permeability (md)	1.99	1.75
Irreducible water saturation (%)	40	39

EXPERIMENTAL SECTION

1. Materials

NaOH (Merck, 99%) and several chemicals including para-alkyl phenol, paraformaldehyde (concentrated source of formaldehyde), and polyamine were purchased from Aldrich and used without further purification for synthesizing the polymeric asphaltene inhibitor. Reservoir water (TDS=147,566 mg/L, SG=1.0945, μ=1.35 cp) and dead oil sample from an oil field in the southwest of Iran were used in the dynamic experiments. The specifications of the oil sample are reported in Table 1. The initial asphaltene content (n-C_7 insoluble) of the oil sample was equal to 1 wt% as measured by IP-143 standard analysis [26]. A sandstone core sample was used for dynamic experiments with the petro-physical properties reported in Table 2. CO_2 gas (>99%) was used for CO_2 injection into the core. N-heptane (Merck, Germany, >99.8%) was used as an asphaltene precipitant in the turbidity test. Toluene (Merck, Germany, >99.8%) was applied for cleaning and removing the deposited asphaltene in the core sample. In addition, toluene and n-heptane were used in IP-143 standard analysis for measuring the weight percent of asphaltene.

2. Synthesis of Polymeric Asphaltene Inhibitor

The SPI was synthesized in a 3-necked round-bottomed flask equipped with a mechanical stirrer, heating system, and temperature controller. The flask was charged with para-alkyl phenol and paraformaldehyde at the 1 : 1 molar ratio. The reaction mixture was degassed by purging with nitrogen. Afterwards, sodium hydroxide was added to the mixture as a base catalyst and the reaction mixture was stirred at 110 °C for 2 h. Water formed from condensation reactions was removed by vacuum during the reaction. The reaction temperature was increased to 140 °C and polyamine was then added to the reaction mixture. The reaction mixture was kept in this condition for additional 1 h under stirring. The obtained product was cooled to the room temperature and used as the asphaltene inhibitor without further treatment.

3. Light Turbidity Method

Light turbidity is a useful method for investigating the stability of asphaltene particles in the presence of inhibitor in crude oil solutions. Turbiscan MA2000 apparatus from Formulaction was used to measure the turbidity of solutions using a pulsed near infrared light source (850 nm) [27,28]. At first, the solutions containing crude oil and different amounts of n-heptane (as asphaltene precipitant) were prepared and shaken for about 1 min. Then, 10 mL of the solutions was poured into a testing glass cell and the precipitation experiments were carried out by Turbiscan apparatus for 15 min running time. Therefore, the lowest concentration of n-heptane that caused the low stability of asphaltene particles in the solution was found. Afterwards, several samples including crude oil and different concentrations of the SPI (250, 500, 1,000, and 2,000 mg/L) were provided and stirred for about 10 min for faster dissolution of inhibitor in the solutions. The resulting concentration of n-heptane in the previous step was added to the solutions and shaken for about 1 min. Then, 10 mL of the solutions was poured into a glass cell and tested by Turbiscan apparatus. Asphaltene precipitation was measured based on the light transmittance variation versus the height of the sample in the cell during of turbidity running time (that was equal to 15 min) [27,28]. The separability number for quantifying the stability of the precipitated asphaltene is defined by Eq. (1). When the separability number is lower than 5, the asphaltene particles have high stability. Between 5 and 10, the asphaltene particles have medium stability in solution and finally; for the values higher than 10, the asphaltene particles have low stability [29].

$$\text{separability number} = \sqrt{\frac{\sum_{i=1}^{n}(x_i - \bar{x})}{n-1}} \quad (1)$$

where x_i is light transmittance (%) at each time, $\bar{x}$ is the average of x_i, n is the number of measurements (n=16 in this study).

The optimum concentration of the SPI for decreasing the asphaltene precipitation was determined as the point that the separability number remained relatively unchanged with increasing the concentration of the SPI in the solution.

4. Core Flooding Setup Preparation

Fig. 1 shows a schematic view of the core flooding setup used in this research to investigate the effect of synthesized polymeric inhibitor on asphaltene deposition during CO_2 injection in a core sample. This setup consists of the following devices:

- Four high pressure stainless steel cylinders for stocking dead oil, CO_2 gas, reservoir water, and toluene.
- A sandstone core from an Iranian oil reservoir in the south west of Iran.
- A stainless steel core holder for holding a core through a sleeve installed horizontally in the setup.
- Positive displacement pumps for injecting the fluid from stocking cylinders through the sandstone core inside a core holder with a constant flow rate.
- A hand pump for applying constant overburden pressure around the sleeve by filling the space between the sleeve and body

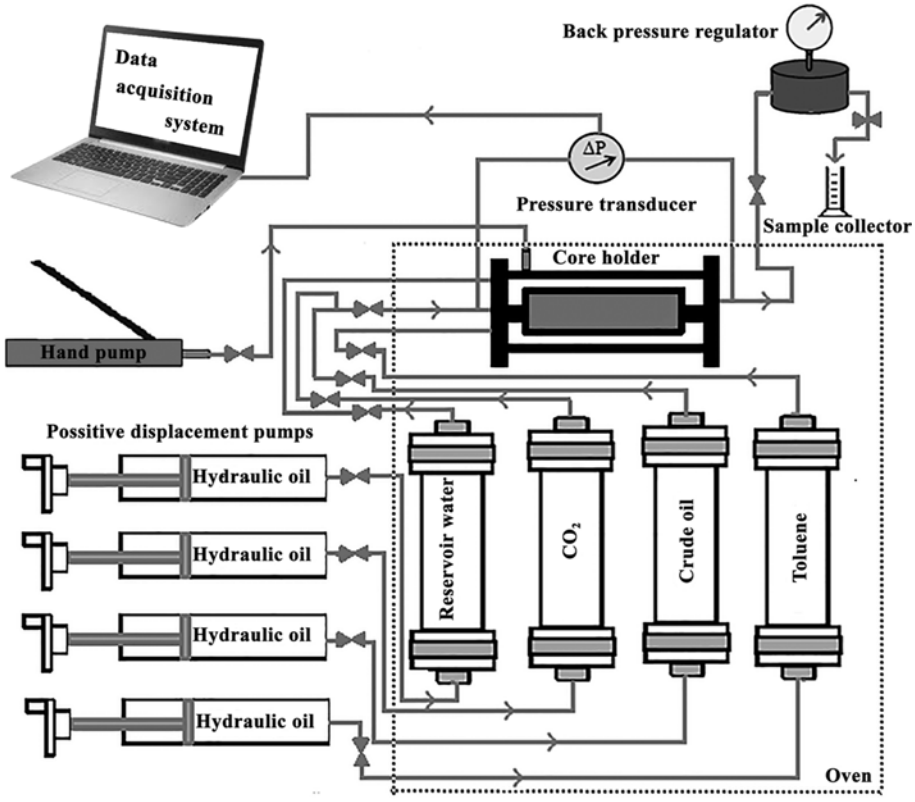

Fig. 1. Schematic view of core flooding setup.

of the core holder with paraffin oil that causes only axial flow in the core sample. The overburden pressure is maintained at 50 bar higher than the injection pressure.

- A pressure transducer for measuring the pressure differences between the inlet and outlet ports of the core holder.
- A back pressure regulator for keeping the constant outlet pressure in the flooding tests.
- A sample collector for collecting the produced fluids from the outlet of the core holder.
- An automated oven for providing a constant temperature during flood injection tests.
- A data acquisition system for recording the resulting data.
- Check valves.

5. CO_2 Injection into a Core Sample

Two sets of dynamic experiments, E1 and E2, were conducted to investigate the formation damage without and with using synthesized asphaltene inhibitor during CO_2 core flooding, respectively. In the experiments, at first, the sandstone core was vacuumed and the reservoir water was imbibed to determine the porosity of the core sample ($Ø_0$≈10%). Second, the reservoir water with a constant flow rate was injected to determine the absolute permeability (k=3.18 md). Third, the reservoir water was displaced by dead oil injection to find irreducible water saturation (swi=40%) and to saturate the core with the dead oil. Fourth, the oil was injected with constant flow rate to determine the initial oil permeability (k_0= 1.99 md). The experiments (E1 and E2) were carried out at 50 °C and 173 bar, which were regulated by the temperature controlled oven and back pressure system, respectively. Based on the CO_2 phase diagram, the CO_2 is supercritical at this temperature and pressure. The pressure of the dynamic experiments was selected higher than minimum miscibility pressure (MMP) for providing miscible CO_2 injection process in E1 and E2 experiments. The relatively high accuracy correlation of Alston et al. applied for the prediction of CO_2-oil MMP as the following equation [30]:

$$MMP = (6.056\times10^{-5})\times(1.8\times T+32)^{1.06} \times(MW_{C5+})^{1.78}\times(X_V/X_L)^{0.136} \quad (2)$$

where MMP is minimum miscibility pressure (bar), T is temperature (°C) and MW_{C5+} is molecular weight of C_{5+} components, X_V is mole fraction of volatile compounds in the oil (C_1, N_2), X_L is the mole fraction of intermediate compounds in the oil (H_2S, CO_2, and C_2-C_4). Based on the dead oil composition in Table 1, the summation of volatile oil fraction consisting of (C_1, N_2) was equal to zero and no H_2S and CO_2 components existed in the dead oil composition. The M_{C5+} was calculated by following mixing rule:

$$MW_{C5+} = \frac{\sum_{i=C_5}^{C_{12+}} x_i MW_i}{\sum_{i=C_5}^{C_{12+}} x_i} \quad (3)$$

So with using the Alston correlation at the test temperature (T= 50 °C), the MMP was found to be 153 bar.

During E1 experiment, the crude oil and CO_2 were co-injected into the core sample by positive displacement pumps at the constant flow rates of 4.7 and 1.3 cm^3/h, respectively. The CO_2 mole percent in the injected fluid was selected about 50 mol%. This value ensured asphaltene precipitation in a core sample because it

was higher than measured static onset point of asphaltene precipitation in this study (≈30 mol%.) and the onset value reported in the literature [31]. Then the pressure differences (ΔP) through the core sample were measured by the pressure transducer and recorded by the data acquisition system at the specified time intervals. The CO_2 injection was continued until ΔP between two ends of the core sample was not increased. During the test, the produced fluids from the outlet of the core holder were collected in the sample collectors to measure the asphaltene content at different pore volumes (PV) of fluid injections. Finally, toluene was being injected continuously to remove the deposited asphaltene formed due to CO_2 injection into the core and to prepare the setup for the second experiment (E2).

In E2 experiment, after reservoir water injection into the core sample, the mixture of dead oil and the optimum concentration of the SPI, which was obtained by light turbidity method, was injected into the core sample for displacing the reservoir water. The irreducible water saturation and initial oil permeability were determined to be 39% and 1.75 md, respectively. Next, co-injection of crude oil/inhibitor mixture and CO_2 gas inside the core was started at the constant injection rates of 4.7 and 1.3 cm^3/h, respectively. The fluid injection in E2 experiment was continued until that the PV became equal to the fluid injection PV of E1 experiment.

The values of permeability through the dynamic experiments (E1 and E2) were calculated by Darcy's law (Eq. (4)).

$$k=\left(\frac{Q*1000}{\Delta P}\right)\left(\frac{L\mu}{A}\right) \tag{4}$$

where k is permeability (md), Q is the summation of the oil and CO_2 flow rates (cm^3/s), ΔP is pressure differences (bar), L is length of the porous media (cm), A is cross-sectional area of the porous media (cm^2), μ is miscible fluid viscosity (cp). The fluid viscosity in E1 and E2 experiments were measured by rolling ball viscometer (Ruska, series 1602) at 173 bar and 50 °C.

The core porosity (Ø) after the specified PV of the fluid injection intervals during E1 and E2 experiments was calculated by the following equations:

$$\text{Ø}=\frac{\text{Initial pore volume}-\text{Deposited asphaltene volume}}{\text{Bulk volume}} \tag{5}$$

$$\text{Deposited asphaltene volume}=\frac{\text{Initial asphaltene mass}-\text{Outlet asphaltene mass}}{\text{Asphaltene density}} \tag{6}$$

The asphaltene density was needed for calculating of core porosity after asphaltene deposition. Asphaltene density at low concentration could be determined by using ideal solution approximation for asphaltene-toluene mixtures. For this purpose, the toluene was added to different amounts of extracted asphaltenes from the crude oil, and the densities of mixtures were measured by pycnometer. The asphaltene density was calculated by using Eqs. (7) to (10) and plotting the inverse mixture density versus asphaltene mass fraction (Fig. 2) [32]:

$$\frac{1}{\rho_M}=\frac{w_T}{\rho_T}+\frac{w_A}{\rho_A} \tag{7}$$

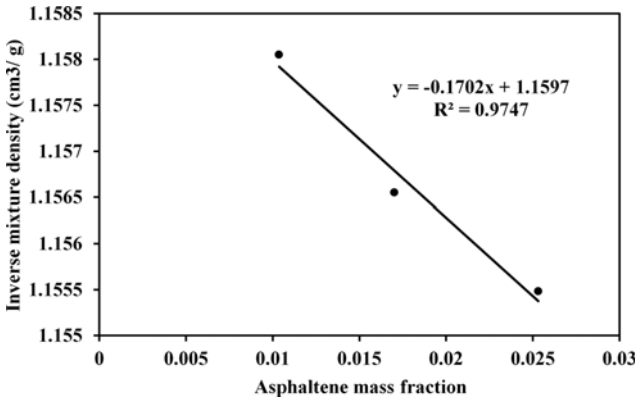

Fig. 2. Asphaltene density measurement.

$$w_T+w_A=1 \tag{8}$$

$$\frac{1}{\rho_M}=\frac{1}{\rho_T}+w_A\left(\frac{1}{\rho_A}-\frac{1}{\rho_T}\right) \tag{9}$$

$$\rho_A=\frac{1}{S+I} \tag{10}$$

where ρ_M, ρ_T and ρ_A are the mixture, toluene and asphaltene densities, respectively. w_T, w_A are toluene and asphaltene mass fractions. S and I are the slope and intercept of the inverse mixture density plot versus asphaltene mass fraction, respectively. Therefore, the asphaltene density was found to be 1.0106 g/cm^3.

RESULTS AND DISCUSSION

1. Characterization of Synthesized Polymeric Inhibitor (SPI)

A Fourier transform infrared spectroscopy (FTIR) test was carried out using a Bruker Equinox 55 spectrophotometer with resolution 4 cm^{-1} in the range of 4,000-400 cm^{-1} to characterize the structure of the synthesized polymeric inhibitor (SPI). Based on the FTIR spectrum of the SPI shown in Fig. 3, wide peaks around 3,280 cm^{-1} and 3,176 cm^{-1} indicated the stretching vibrations of O-H groups of phenol and N-H groups of polyamine, respectively [33,34]. The

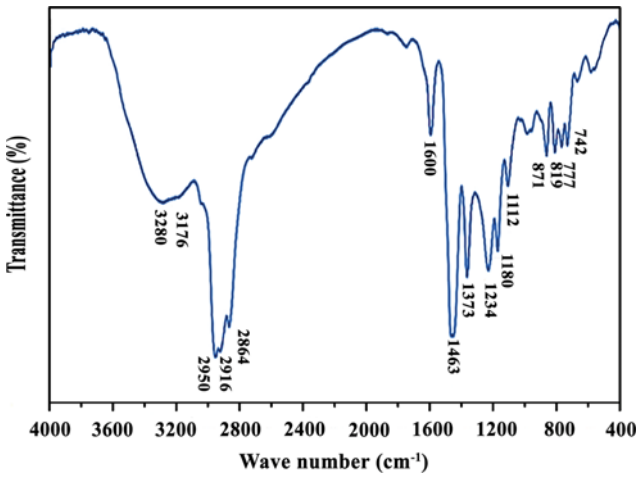

Fig. 3. FTIR spectra of synthesized polymeric inhibitor (SPI).

Table 3. Stability results for different concentrations of oil and n-heptane

Test no.	Oil (mL)	N-heptane (mL)	Separability number	Stability condition
1	1	5	0.7	High
2	1	30	8.2	Medium
3	1	35	12	Low

absorption bands from 2,700 to 3,000 cm^{-1} referred to aliphatic C-H stretching vibrations. Two peaks around 1,600 and 1,463 cm^{-1} indicated aromatic C=C bending in benzene rings. The peak at 1,373 cm^{-1} showed CH_3 bending. The absorption bands from 900 to 1,200 cm^{-1} displayed C-C stretching vibrations. The series of weak peaks in the region 700-900 cm^{-1} indicated the aromatic C-H out-of-plane bending [35,36].

The molecular weight of the polymer was determined by gel permeation chromatography (GPC). The weight-average molecular weight (Mw) was measured as 17,700 g/mol.

2. Turbidity Test Results

The crude oil samples with different amounts of n-heptane were tested by Turbiscan apparatus to find the asphaltene stability in the solution. The results of separability number are presented in Table 3. Based on the results, the solution containing n-heptane and crude oil in the ratio of 35 : 1 (vol/vol) was selected as the lowest ratio that caused the low stability of asphaltenes in the solutions.

Next, solutions with different concentrations of the SPI in the oil were prepared and n-heptane was added with the ratio of 35 : 1 (vol/vol) to the solutions. The resulting samples were tested by Turbiscan apparatus for 15 min running time. The separability numbers and stability conditions of asphaltene particles are reported in Table 4. The results showed that the asphaltene particles had high stability (separability number <5) when the SPI at different concentrations was added to the solution. It was found that, by increasing the concentration of the SPI to higher than 500 mg/L, no more changes were observed in values of separability number. Therefore, 500 mg/L was selected as the optimum concentration of the SPI for inhibition of asphaltene precipitation in the solution.

In addition, the light transmittance along the cell was recorded at 1 min time intervals. Fig. 4(a), (b) shows the curves of percentage transmittance (%T) versus height of the samples in the cell, without and with using 500 mg/L inhibitor, respectively. Each curve related to a specified time shown on right hand side of Fig. 4.

At first, the transmittance value was equal to zero, because the sample was dark and no light could be transmitted through the solution. Afterwards during the time, the precipitation and settling of asphaltene happened and the light could transmit through the upper section of the cell [27]. In the case of using the inhibitor, the transmittance value remained close to zero for higher heights of the samples in the cell with the comparison of the case without using the inhibitor, which could indicate that the asphaltene particles remained well dispersed in the solution in the presence of the polymeric inhibitor. Also, it can be observed that the values of transmittance in Fig. 4(a) increased sharply to about 40% as a function of time. In this case, the amount of asphaltene in the solution decreased and, consequently, sedimentation occurred during 15 min, so more light could be transmitted through the solution. However, Fig. 4(b) shows that the transmittance was relatively constant during turbidity running time and the transmittance value increased by just about 10% at the end of the test, which could be due to the delay and decrease of asphaltene precipitation in the solution when the SPI was used.

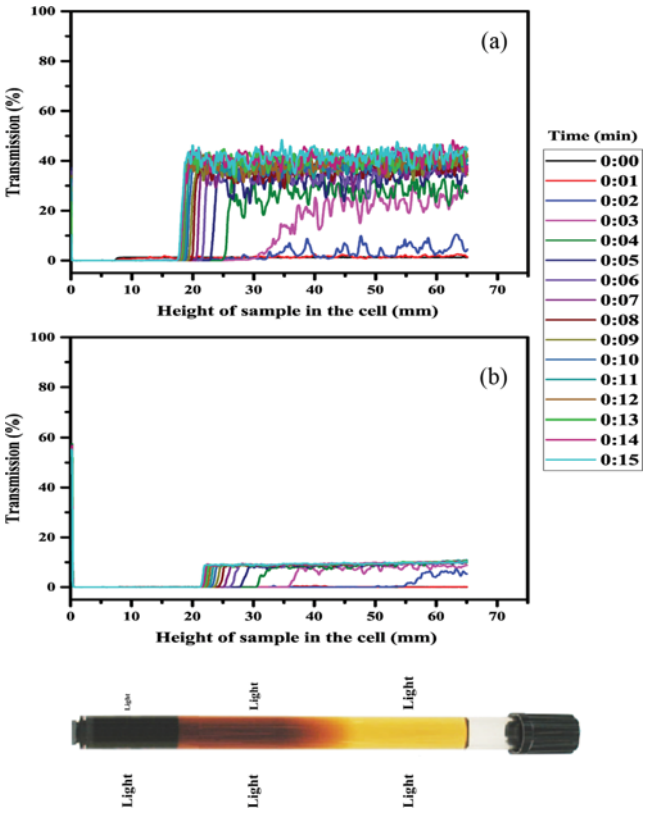

Fig. 4. Curves of transmittance percent (%T) versus height of sample in the testing cell at different times from 1 to 15 min (a) without using inhibitor and (b) with using 500 mg/L of SPI.

Table 4. Stability results for adding different concentrations of SPI

Test no.	SPI concentration (mg/L)	Separability number	Stability condition
1	250	3.5	High
2	500	2.1	High
3	1000	1.9	High
4	2000	1.8	High

3. Effect of SPI on Permeability Reduction in CO_2 Core Flooding

Two dynamic experiments were conducted for investigating the formation damage during CO_2 injection into the porous media. The first experiment (E1) included the co-injection of miscible CO_2 and dead oil into the sandstone core at 173 bar and 50 °C. But, in the second experiment (E2), the mixture of dead oil and optimum concentration of the SPI (500 mg/L) was co-injected with CO_2 for studying the impacts of the SPI on asphaltene deposition. During the experiments, the ΔP values between two ends of the

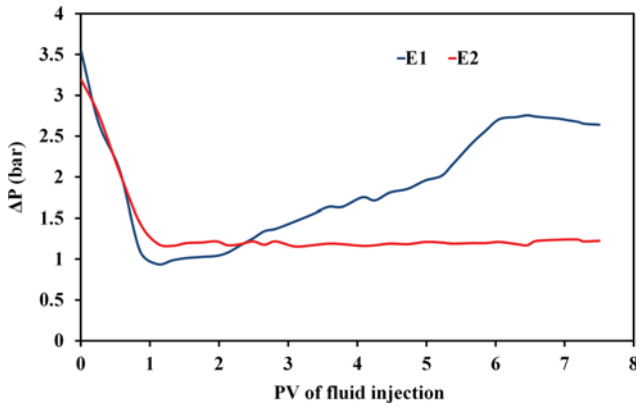

Fig. 5. Recorded ΔP between the two ends of the core holder.

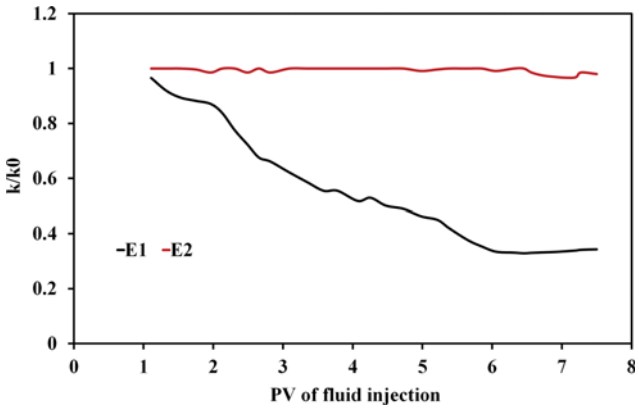

Fig. 6. Permeability reduction during CO_2 injection in a core sample with and without the use of SPI.

core holder were measured by the pressure transducer. Fig. 5 shows the ΔP changes versus pore volume (PV) of the fluid mixture injections. In both experiments (E1 and E2) the ΔP decreased until about 1 PV of fluid injection. Co-injection of CO_2 and oil into the core sample, which was previously saturated with the oil, caused a decrease in the fluid viscosity. Consequently, ΔP decreased until miscibility occurred and a single phase was formed in the core sample. In E1 experiment, a sharp increase in ΔP values after 1.5 PV of fluid injection indicated the formation damage. With the injection of CO_2 into the core sample, the oil equilibrium condition changed and caused precipitation and deposition of asphaltene on the core.

As long as the asphaltene deposition continued in porous media, the area for fluid stream was reduced and the velocity of fluid increased due to constant flow rate of fluids in the core. So based on the constant outlet pressure, which was regulated by back pressure system, and the Bernoulli equation, the inlet pressure decreased, and consequently the ΔP along the core increased.

However, in E2 experiment, after 1 PV of fluid injection, ΔP was relatively constant and no increase was observed in Fig. 5. Therefore, the constant values of pressure differences during CO_2 core flooding indicated good inhibition effect of the SPI on the asphaltene deposition.

The oil permeabilities after miscibility were calculated using Darcy's law equation by applying the recorded pressure differences at flow rate of miscible fluid (6 cm^3/h), and by measuring the viscosity of the miscible fluid at operating temperature and pressure in E1 and E2 (μ=1.41 cp in E1 and μ=1.63 cp in E2).

According to the literature [37,38], while miscibility has not occurred, the fluid composition is unknown and a reliable value for the fluid viscosity cannot be estimated. Therefore, the permeability reduction results after miscibility (>1 PV of fluid injections) are demonstrated in Fig. 6. It can be observed that the permeability ratio in E1 was reduced to 0.3. Based on the Darcy's law, the permeability is a function of ΔP. So the permeability ratio along the core decreased with increasing the ΔP as shown in Figs. 5 and 6.

The ΔP and permeability ratio plots (Figs. 5 and 6) have several parts. These parts indicate different mechanisms of asphaltene deposition including surface deposition, pore throat plugging and entrainment of asphaltene deposited [39]. Surface deposition mechanism, including deposition of asphaltene particles on the surface of the pores, causes gradual pore plugging and low permeability reduction in porous media [39]. In E1, this mechanism occurred at initial PV of fluid injection. Pore throat plugging mechanism, including mechanically plugging the pore throats with accumulation of asphaltene particles, results in high permeability reduction in porous media [39]. In E1, this mechanism occurred between 1 and 6 PV of fluid injection. However, entrainment of asphaltene deposited, including removing away the deposited asphaltene by the fluid stream, occurs as a third mechanism when the fluid velocity becomes higher than critical velocity. So the permeability ratio temporarily increases in the porous media [39]. In E1, this mechanism was dominant after 6 PV of fluid injection. Therefore, a little increasing of permeability after 6 PV of fluid injection implies that there is no more asphaltene deposition occurrence in a core sample due to entrainment of asphaltene deposited.

In E2, the permeability ratio values remained constant during all PVs of the fluid injections. The results of E1 experiment confirmed that the asphaltene deposition occurred during CO_2 injection in porous media. Therefore, relatively constant ΔP value and permeability ratio throughout the E2 experiment confirmed no occurrence of asphaltene deposition in a core sample because of using inhibitor. So it can be concluded that the SPI can inhibit the asphaltene deposition during CO_2 injection in the core sample. Hydrogen bonds between phenol acidic groups in structure of the SPI and asphaltene aggregates and π-π interactions between their aromatic rings have a good effectiveness on asphaltene stabilization. Also, long alkyl chains of the SPI can help disperse any formed asphaltene aggregates. On the other hand, basic amine in inhibitor's structure causes interactions between band organic acids in oil and prevents asphaltene deposition [40].

4. Effect of SPI on Outlet Asphaltene Content in CO_2 Core Flooding

The produced fluids from the outlet of the core holder were collected in the sample collectors at the specified PV of fluid injection interval. Then, the asphaltene wt% of the outlet fluids was measured by IP-143 standard analysis [26] and the results are shown in Fig. 7. It was found that the asphaltene content of the outlet fluid without inhibitor (E1) decreased from initial concentration of

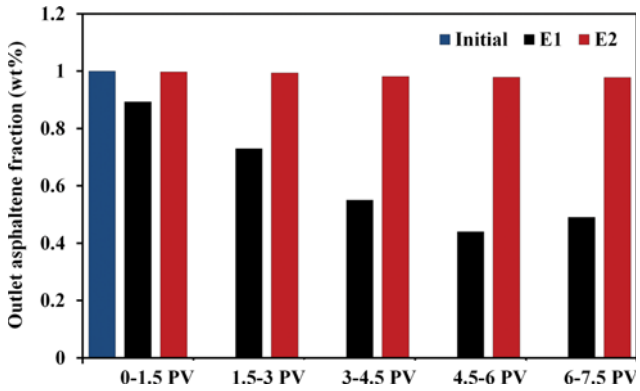

Fig. 7. Outlet fluid Asphaltene wt% from CO_2 injection in a core sample with and without the use of SPI.

asphaltene (1 wt about 0.49 wt% at the end of the test. It can be seen in E1, within the range of 0 to 1.5 PV of the fluid injections, the outlet asphaltene content decreased by about 10% due to asphaltene deposition on the core surfaces. Afterwards, until 6 PV of the fluid injections, the outlet asphaltene content was severely decreased by about 56% in comparison to the initial asphaltene concentration. High decrease of asphaltene concentration referred to high asphaltene deposition and pore plugging of the core during CO_2 injection. Finally, with stopped increasing of ΔP after 6 PV, the outlet asphaltene content increased slightly, which was due to asphaltene entrainment phenomenon during core flooding. However, in E2 experiment, the amounts of outlet asphaltene were relatively constant (≈1 wt%) and did not significantly decrease from the initial asphaltene content, which could indicate lack of asphaltene deposition in the core sample.

5. Effect of SPI on Porosity Reduction in CO_2 Core Flooding

The results of outlet asphaltene wt% were applied to calculate the porosity reduction. The ratio of core porosity to initial porosity and deposited asphaltene wt% versus PV of fluid injections are shown in Fig. 8. The deposited asphaltene wt% was obtained by subtracting the amount of outlet asphaltene from the initial asphaltene content. It could be concluded that an increase of the asphaltene deposition reduced porosity ratio ($Ø/Ø_0$) to about 0.97 in E1

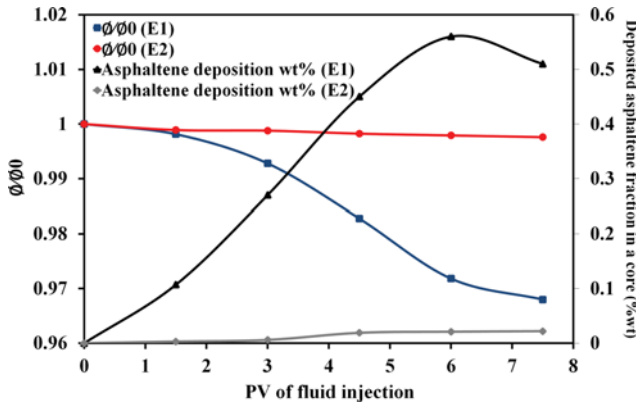

Fig. 8. Porosity reduction and asphaltene deposition wt% during CO_2 injection in a core sample with and without the use of SPI.

experiment. Decrease in the asphaltene deposition value at the last PV of fluid injection in E1 indicated the entrainment of asphaltene during core flooding. Note that, in E1, the porosity reduction was much lower than the results of permeability reduction, which might be due to forming asphaltene deposition in local positions in the core, instead of along the core [32]. But, in E2, negligible asphaltene deposition was observed in the presence of the synthesized polymeric inhibitor that caused no porosity reduction during the CO_2 injection into the core sample.

CONCLUSIONS

A new synthesized polymeric inhibitor (SPI) on asphaltene deposition was investigated by light turbidity method. The results showed that the asphaltene particles had high stability when the SPI was added to the solution. The optimum concentration of the inhibitor for delaying the asphaltene deposition in the oil solution was found to be 500 mg/L. The inhibition effects of the SPI on asphaltene deposition during CO_2 injection into the sandstone core were also investigated at high pressure and high temperature. According to the experimental results of the CO_2 injection, it could be concluded that the synthesized polymeric inhibitor could inhibit the asphaltene deposition in the porous media. This result was obtained according to negligible permeability reduction and no more changes in outlet fluid asphaltene contents at different pore volume of fluid injections in the dynamic experiment E2. The strong intermolecular interactions between the polar groups of the SPI and the precipitated asphaltenes prevented the self-association of asphaltene particles and inhibited them from aggregation in the solution. Therefore, the SPI could be used as an effective inhibitor with good performance on inhibition of asphaltene deposition.

REFERENCES

1. K. Narayan and B. Walsh, *Fuel*, **67**, 215 (1988).
2. X. Wang and Y. Gu, *Ind. Eng. Chem. Res.*, **50**, 2388 (2011).
3. K. Babu, N. Pal, V. K. Saxena and A. Mandal, *Korean J. Chem. Eng.*, **33**, 711 (2016).
4. M. S. Benzagouta, I. M. AlNashef, W. Karnanda and K. Al-Khidir, *Korean J. Chem. Eng.*, **30**, 2108 (2013).
5. H. Son, H. Kim, G. Lee, J. Kim and W. Sung, *Korean J. Chem. Eng.*, **31**, 338 (2014).
6. S. Kwon and W. Lee, *Korean J. Chem. Eng.*, **29**, 750 (2012).
7. P. Zanganeh, S. Ayatollahi, A. Alamdari, A. Zolghadr, H. Dashti and S. Kord, *Energy Fuels*, **26**, 1412 (2012).
8. D. Borton, D. S. Pinkston, M. R. Hurt, X. Tan, K. Azyat, A. Scherer, R. Tykwinski, M. Gray, K. Qian and H. I. Kenttämaa, *Energy Fuels*, **24**, 5548 (2010).
9. J. S. Buckley and J. Wang, *J. Petrol. Sci. Eng.*, **33**, 195 (2002).
10. C.-L. Chang and H. S. Fogler, *Langmuir*, **10**, 1749 (1994).
11. T. A. Al-Sahhaf, M. A. Fahim and A. S. Elkilani, *Fluid Phase Equilib.*, **194**, 1045 (2002).
12. I. H. Auflem, T. Havre and J. Sjöblom, *Colloid. Polym. Sci.*, **280**, 695 (2002).
13. L. C. R. Junior, M. S. Ferreira and A. C. da Silva Ramos, *J. Petrol. Sci. Eng.*, **51**, 26 (2006).

14. L. Goual, M. Sedghi, X. Wang and Z. Zhu, *Langmuir*, **30**, 5394 (2014).
15. M. Boukherissa, F. Mutelet, A. Modarressi, A. Dicko, D. Dafri and M. Rogalski, *Energy Fuels*, **23**, 2557 (2009).
16. W. K. Stephenson, B. D. Mercer and D. G. Comer, US Patent, 5143594 A (1992).
17. D. Miller, M. Feustel, A. Vollmer, R. Vybiral and D. Hoffmann, US Patent, 6180683 B1 (2001).
18. P. J. Breen, US Patent, 6313367 B1 (2001).
19. M. F. Wilkes and M. C. U. S. Davies, Patent Application, 2008/0096772 (2008).
20. Y.-F. Hu and T.-M. Guo, *Langmuir*, **21**, 8168 (2005).
21. M. Karambeigi and R. Kharrat, *Pet. Sci. Technol.*, **32**, 1327 (2014).
22. H. H. Ibrahim and R. O. Idem, *Energy Fuels*, **18**, 743 (2004).
23. L. A. Alcázar-Vara, L. S. Zamudio-Rivera, E. Buenrostro-González, R. Hernández-Altamirano, V. Y. Mena-Cervantes and J. F. Ramírez-Pérez, *Ind. Eng. Chem. Res.*, **54**, 2868 (2015).
24. S. Ghazvini, M. Omidkhah Nasrin and M. Nikazar, *J. Oil Gas Petrochem. Technol.*, **1**, 57 (2014).
25. S. I. Hashemi, B. Fazelabdolabadi, S. Moradi, A. M. Rashidi, A. Shahrabadi and H. Bagherzadeh, *Appl Nanosci.*, **6**, 71 (2016).
26. Standard Test Method for Determination of Asphaltenes (Heptane Insolubles) in Crude Petroleum and Petroleum Products, ASTMD6560-00 (2005).
27. K. Kraiwattanawong, H. S. Fogler, S. G. Gharfeh, P. Singh, W. H. Thomason and S. Chavadej, *Energy Fuels*, **23**, 1575 (2009).
28. J. Pereira, J. Delgado-Linares, A. Briones, M. Guevara, C. Scorzza and J.-L. Salager, *Pet. Sci. Technol.*, **29**, 2432 (2011).
29. Standard Test Method for Measuring n-Heptane Induced Phase Separation of Asphaltene-Containing Heavy Fuel Oils as Separability Number by an Optical Scanning Device, ASTMD7061-12 (2012).
30. R. B. Alston, G. P. Kokolis and C. F. James, *Soc. Petrol. Eng. J.*, **25**, 268 (1985).
31. P. Bahrami, R. Kharrat, S. Mahdavi, Y. Ahmadi and L. James, *Korean J. Chem. Eng.*, **32**, 316 (2015).
32. M. Bagheri, R. Kharrat and C. Ghotby, O*il Gas Sci. Technol.*, **66**, 507 (2011).
33. A. Tóth, K. Szentmihályi, Z. Keresztes, I. Szigyártó, D. Kováčik, M. Černák and K. Kutasi, *Open Chem.*, **13**, 557 (2015).
34. H. Jiang, X. Sun, M. Huang, Y. Wang, D. Li and S. Dong, *Langmuir*, **22**, 3358 (2006).
35. M. J. Iglesias, A. Jiménez, F. Laggoun-Défarge and I. Suarez-Ruiz, *Energy Fuels*, **9**, 458 (1995).
36. R. Bodirlau, C. A. Teaca and I. Spiridon, *BioResources*, **4**, 1285 (2009).
37. N. I. Papadimitriou, G. E. Romanos, G. Ch. Charalambopoulou, M. E. Kainourgiakis, F. K. Katsaros and A. K. Stubos, *J. Petrol. Sci. Eng.*, **57**, 281 (2007).
38. H. Bagherzadeh, M. Ghazanfari, R. Kharrat and D. Rashtchian, *Energy Source. Part A*, **36**, 591 (2014).
39. A. Danesh, D. Krinis, G. D. Henderson and J. M. Peden, *J. Petrol. Sci. Eng.*, **2**, 167 (1989).
40. M. A. Kelland, *Production chemicals for the oil and gas industry*, CRC Press (2014).